

Inferring ecological interactions from time series data using neural ordinary differential equations fitted by gradient matching

Willem Bonnaffé^{1,2}, Ben Sheldon¹, & Tim Coulson²

1. Edward Grey Institute of Field Ornithology, Department of Zoology, Oxford University, Zoology Research and Administration Building, 11a Mansfield Road, Oxford OX1 3SZ

2. Ecological and Evolutionary Dynamics Lab, Department of Zoology, Oxford University, Zoology Research and Administration Building, 11a Mansfield Road, Oxford OX1 3SZ

Emails: willem.bonnafe@stx.ox.ac.uk; tim.coulson@zoo.ox.ac.uk

Running title: Repeatable interactions and dynamics

Keywords: Artificial Neural Networks; Ecological Dynamics; Ecological interactions; Geber Method; Neural Ordinary Differential Equations; Ordinary Differential Equations; Prey-predator dynamics; Time series analysis; Rotifers; Microcosm;

Specifications: 140 words in abstract; 7071 words in text; 40 references; 5 figures; 1 table

Contact: Willem Bonnaffé, 61 St Giles, Pusey House, St Cross College, Oxford, OX1 3LZ, UK (w.bonnafe@gmail.com)

Statement of authorship: Willem Bonnaffé designed the method, performed the analysis, wrote the manuscript; Ben Sheldon provided input for the manuscript, commented on the manuscript. Tim Coulson led investigations, provided input for the manuscript, commented on the manuscript.

Abstract

Generalisation of dynamical processes across natural systems is difficult because they are complex and hard to observe. The hope is that generalisation may be achieved by adequately modelling the complexity of systems, and observe them in sufficient detail. We investigate this by looking at the consistency of ecological interactions across three replicates of a three-species prey-predator system, well-observed in an artificial environment, using neural ordinary differential equations. We find that dominant interactions are consistent across the replicates, while weaker interactions are not, leading to different dynamical patterns across replicated systems. Our study hence suggests that generalisation of dynamical processes across systems may not be possible, even in simpler systems in ideal monitoring conditions. This is a problem because if we are not able to make generalisations in a simple artificial system, how can we make generalisation in the real world?

1 Introduction

The repeatability of ecological and evolutionary dynamics varies widely across systems and species. Sticklebacks from different lakes in Canada have independently evolved to a similar river morph phenotype (Thompson, Taylor, and Mcphail 1997). In guppies, four replicated populations located in different streams in Trinidad evolved the same low-predation phenotype (Reznick, Bryga, and Endler 1990). Multiple studies in experimental microcosms, particularly in rotifer populations, have shown that population dynamics were broadly repeatable (Yoshida et al. 2003; Yoshida et al. 2007; Becks et al. 2010; Becks et al. 2012; Hiltunen et al. 2013). Overall, this demonstrated that ecological and evolutionary dynamics may be repeatable across different instances of the same system, at least qualitatively. This was a fascinating finding given the complexity of the mechanisms involved and the subtle variations in environmental conditions across the different populations.

These systems hinted at the possibility for identifying global, generalisable, dynamical models. In practice, however, generalising dynamics and dynamical processes (i.e. functional representations describing which and how state variables affect each other and determine system dynamics) across natural systems has proven difficult (Lawton 1999). First, even if the dynamical patterns, and their outcomes, may appear to be conserved across similar systems, they may be underpinned by different processes. For instance, the evolution of the sticklebacks to highly similar river-adapted phenotypes has been shown to be underpinned by radically different genetic alterations (Raeymaekers et al. 2017). Second, it is often unclear whether quantitative differences across replicated systems

21 arise from pure stochasticity (Dallas et al. 2021), observation error (De Meester et al. 2019), or
22 deterministic changes in the dynamical processes. Finally, the complexity of biological processes
23 themselves (Adamson and Morozov 2013), differences in genetic and environmental contexts, may
24 prevent the identification of a suitable dynamical model. For example, Becks and colleagues found
25 that differences in the initial amount of genetic variation in otherwise identical rotifer populations
26 led to subtle changes to the dynamics (Becks et al. 2010). Different access to seed supplies can
27 modify the strength of the interaction between a plant and its herbivore, leading to either stable or
28 oscillatory dynamics (Bonsall, Van Der Meijden, and Crawley 2003). Differences in temperature
29 can alter the ecological interaction structure of entire ecosystems (Shurin et al. 2012; Bonnaffé
30 et al. 2021). Because of this, vital rates are often found to be inconsistent in time (Gross, Ives, and
31 Nordheim 2005; Adamson and Morozov 2013), and space (e.g. Gamelon et al. 2019). Overall, a
32 growing body of evidence shows that generalisation of dynamical processes across similar natural
33 systems often fails (Lawton 1999, e.g. Kendall et al. 2005; Demyanov, Wood, and Kedwards 2006;
34 Ezard, Côté, and Pelletier 2009).

35 So how could repeatable dynamics arise across multiple instances of the same system? We would
36 expect dynamics to be repeatable if the components of the system (e.g. species), as well as interac-
37 tions between components, are conserved. For this, populations should have similar distributions
38 for the traits that underpin these interactions, and should further share the same environmental con-
39 ditions, across instances. While this is unreasonable to expect from a natural system, it may be
40 achievable in an artificial setting. In such a setting, it is possible to understand the structure of

41 the system, to control the environment, and to reduce observation error. So if we fail to identify
42 and generalise dynamical models in natural systems, perhaps we may be able to do so in artificial
43 systems.

44 In spite of this there are few studies that have attempted to characterise the generalisability of
45 dynamics across replicated systems in a laboratory setting. In such a setting, idiosyncrasies in pop-
46 ulation dynamics can arise from (1) variations in ecological interactions and individual processes,
47 as a result of evolution (e.g. Yoshida et al. 2003), or stochasticity (Dallas et al. 2021), (2) variations
48 in initial conditions due to the experimental setting (Yoshida et al. 2003; Becks et al. 2010; De
49 Meester et al. 2019), and (3) the complexity of the system which can lead to large changes in sys-
50 tem dynamics with small changes in the system state and structure (Adamson and Morozov 2013).

51 Two studies, one in aphids and the other in rotifers, found substantial variation in vital rates across
52 replicated populations, by fitting a stage-structured population ODE model to population dynamics
53 time series data (Bruijning, Jongejans, and Turcotte 2019; Rosenbaum et al. 2019). These studies
54 hint that generalisability of population dynamical processes may not be possible because of in-
55 trinsic population structure and evolution, even in virtually identical populations hosted in artificial
56 environments.

57 We identified three gaps in the literature. First, this kind of evidence remains scarce, due in part
58 to the fact that dynamical modelling approaches guided by empirical data are still not widespread
59 (Pontarp, Brännström, and Petchey 2019). Second, most of these studies relied on parametric
60 frameworks, which impose arbitrary pre-determined forms for the dynamical processes at play, so

61 that their model may not capture properly the complexity of the dynamics of these populations (Jost
62 and Ellner 2000; Adamson and Morozov 2013; Bonnaffé, Sheldon, and Coulson 2021). Finally,
63 most studies usually analyse dynamics in single-species systems, but not multi-species systems,
64 such as those with intraguild predation, which are more biologically realistic scenarios (Hiltunen
65 et al. 2013). Further studies are consequently required to investigate the consistency of dynamical
66 processes in simple multi-species and well-observed systems, to conclude about the generalisability
67 of population dynamics across systems.

68 Our aim in this study is to provide an assessment of the repeatability of dynamical processes across
69 different instances of a realistic multi-species system hosted in a well-observed environment. We
70 do this by quantifying the direction, strength, and consistency of interactions in time and across
71 replicates of a three-species microcosm in an experimental setting. We hypothesise that if the
72 system is (1) simple enough, (2) well-observed, (3) in a controlled environment, then dynamical
73 effects/interactions should be broadly consistent in time and across replicates, hence allowing for
74 generalisation of dynamics across systems. We consider three replicates of a three-species system,
75 consisting in a prey (algae), intermediate-predator (flagellate), and top-predator (rotifer). The algae
76 is consumed by the flagellate and rotifer, and the flagellate is consumed by the rotifer. We use
77 three replicated system runs from a study by Hiltunen and colleagues which feature sequential
78 oscillations of the density of the three species (Hiltunen et al. 2013). We analyse the time series
79 with neural ordinary differential equations (Bonnaffé, Sheldon, and Coulson 2021), which allows
80 us to approximate non-parametrically population growth rates, and quantify the direction, strength,

81 and consistency of inter- and intra-specific effects on the growth of each population. We find that
82 the interaction between the rotifer and algae is consistent throughout time and across replicates,
83 while the interaction between the flagellate and the two other species is not. Our study suggests
84 that dynamical processes may sometimes not be consistent and generalisable across systems, even
85 when they are as close to identical as experimentation permits. We discuss these results and hint at
86 the underlying impact of evolution driving differences in these systems.

87 **2 Material and Methods**

88 **2.1 Method overview**

89 We aim to provide a nonparametric method for estimating ecological interactions from time series
90 data of species density. We do this by approximating the dynamics of each species with neural
91 ordinary differential equations (NODEs, Bonnaffé, Sheldon, and Coulson 2021). We then compute
92 ecological interactions as the sensitivity of these dynamics to a change in the respective species
93 densities.

94 **2.2 Neural ordinary differential equation**

95 A NODE is a class of ordinary differential equation (ODE) that is partly or entirely defined as an
96 artificial neural network (ANN). They are useful to infer dynamical processes non-parametrically
97 from time series data (Bonnaffé, Sheldon, and Coulson 2021). We choose NODEs over standard
98 statistical approaches because they offers two advantages. The first is that NODEs approximate the

99 dynamics of populations non-parametrically. NODEs are therefore not subjected to incorrect model
 100 specifications (Jost and Ellner 2000; Adamson and Morozov 2013). This provides an objective
 101 estimation of the inter-dependences between state variables. The second advantage is that it is a
 102 dynamical systems approach. So that the approach includes lag effects through interacting state
 103 variables, not only direct effects between them.

104 For the sake of simplicity, we first consider a two-species NODE system:

$$\begin{cases} \frac{dR}{dt} = r_R(R, N, \beta_R)R \\ \frac{dN}{dt} = r_N(R, N, \beta_N)N \end{cases} \quad (1)$$

105 where dR/dt and dN/dt denote the change in the density of prey ($R \in \mathcal{R}^+$), and predator ($N \in \mathcal{R}^+$),
 106 in continuous time. The per-capita growth rates r_R and r_N are non-parametric functions of the
 107 density of each species. The shape of the non-parametric functions is controlled by the parameter
 108 vectors β_R and β_N .

109 Traditionally, each non-parametric function is defined as an ANN function of the state variables.
 110 The most common class of ANN used for NODEs are single layer perceptrons (SLPs):

$$r_N(R, N, \beta_N) := \beta_0 + \sum_{i=1}^I \beta_i f_{\sigma}(\beta_{i0} + \beta_{i1}R + \beta_{i2}N) \quad (2)$$

111 which map the density of each species R and N to the corresponding per-capita growth rate through
 112 a single hidden layer. The parameter vector β_R and β_N are the weights of the connections in the

113 SLPs. SLPs can be viewed as weighted sums of basis functions f_{σ} . More details regarding these
114 models can be found in our previous work (Bonnaffé, Sheldon, and Coulson 2021).

115 **2.3 Fitting NODEs by gradient matching**

116 This section describes how to estimate the parameters β of the NODE system given a set of time
117 series. In previous work, we developed a simulation-based approach to fit NODE systems to time
118 series data (Bonnaffé, Sheldon, and Coulson 2021). We would first simulate the NODE system over
119 the entire time series. Then we would compute the error between the predictions of the NODE
120 model and the observations. Finally, we would change the weights of the NODEs to minimise
121 this error. There are two caveats with this approach. The first caveat is that the NODE system
122 has to be simulated over the entire range of the data at every step of the optimisation. This step
123 is computationally expensive to perform. Second, the simulation prevents the computation of
124 gradients of the posterior distribution of the model. This prevents the use of efficient gradient
125 descent approaches.

126 Instead, we propose to use a *gradient matching* approach to fit NODEs, which relies on data in-
127 terpolation to approximate states and dynamics. The method we propose here is derived from the
128 *gradient matching* approach that Ellner and colleagues developed to fit ODEs (Ellner, Seifu, and
129 Smith 2002; Wu, Fukuhara, and Takeda 2005). We proceed in three steps, presented graphically
130 in Fig. 1 and detailed in the following sections. First, we interpolate the time series data and
131 dynamics of each species in the system. Second, we fit each NODE directly to interpolated dy-

namics, thereby avoiding the simulation step of the previous method. This amounts to fitting the interpolated per-capita growth rates with ANNs taking as input the density of each population. Finally, we derive the direction and strength of ecological interactions by computing the intra- and inter-specific sensitivities and contributions.

Interpolating the data

We interpolate the time series and differentiate it with respect to time in order to approximate the dynamics of the system. We perform the interpolation via non-parametric regression of the interpolating function on the time series data

$$\varepsilon_{N,t}^{(o)} = N_t - \tilde{N}(t, \Omega_N) \quad (3)$$

where $\varepsilon_{N,t}^{(o)}$, the observation error, is defined as the difference between N_t , the observed value of the variable at time t , and $\tilde{N}(t, \Omega_N)$, the value predicted by the interpolating function. The interpolating function is chosen to be a SLP with sinusoid activation functions

$$\tilde{N}(t, \Omega_N) = \exp \left\{ \sum_{i=1}^I \omega_{i0} \sin(\pi(\omega_{i1} + \omega_{i2}t)) \right\} \quad (4)$$

where $\tilde{N}(t, \Omega_N)$ is the interpolated state variable, defined as a weighted sum of sinusoid functions of time. The interpolation parameter vector Ω_N contains the weights ω_{i0} , ω_{i1} , and ω_{i2} which control the amplitude, shift, and frequency of the oscillations in the time series, respectively. We found

146 sinusoid activation functions to be most efficient for interpolating population dynamics compared
 147 to other functions (such as sigmoid, hyperbolic). Following this approach we obtain directly an
 148 approximation of the dynamics of the state variable by differentiating the SLP with respect to
 149 time

$$\frac{\partial}{\partial t} \tilde{N}(t, \Omega_N) = \sum_{i=1}^I \omega_{i0} \pi \omega_{i2} \cos(\pi(\omega_{i1} + \omega_{i2}t)) \exp \left\{ \sum_{i=1}^I \omega_{i0} \sin(\pi(\omega_{i1} + \omega_{i2}t)) \right\} \quad (5)$$

150 as well as an analytical expression of the interpolated per-capita growth rate of the populations, by
 151 combining equation (4) and (5)

$$\tilde{r}_N(t, \Omega_N) := \frac{1}{\tilde{N}} \frac{\partial \tilde{N}}{\partial t} = \sum_{i=1}^I \omega_{i0} \pi \omega_{i2} \cos(\pi(\omega_{i1} + \omega_{i2}t)) \quad (6)$$

152 **Fitting NODEs to the interpolated data**

153 The second step is to match the NODE system (1) to the interpolated dynamics, given the interpo-
 154 lated state variables. Thanks to the interpolation of the data, this simply amounts to performing a
 155 non-parametric regression of the NODE approximation of the per-capita growth rate (equation 2)
 156 on the interpolated per-capita growth rate (equation 6)

$$\varepsilon_{N,t}^{(p)} = \tilde{r}_N(t, \Omega_N) - r_N(\tilde{R}, \tilde{N}, \beta_N) \quad (7)$$

157 where the process error, $\varepsilon_{N,t}^{(p)}$, is defined as the difference between the interpolated growth rate \tilde{r}_N
 158 and the NODE approximation r_N .

159 **Statistical modelling approach**

160 Overall, fitting the NODE system (1) comes down to two steps. First, we interpolate the data by
 161 finding the parameter vector Ω that minimises the observation error $\varepsilon^{(o)}$ in equation (3). Second, we
 162 fit the NODE per-capita growth rate by finding the parameter vector β that minimises the process
 163 error $\varepsilon^{(p)}$ in equation (7).

164 The fitting of the models is performed in a Bayesian framework, considering normal error structure
 165 for the residuals, and normal prior density distributions on the parameters

$$p(\theta|\mathcal{D}) \propto p(\mathcal{D}|\theta)p(\theta) \quad (8)$$

166 where θ is the parameter vector of the model, and \mathcal{D} the evidence, namely the data that the model
 167 is fitted to. Assuming a normal likelihood for the residuals given the evidence we get

$$p(\mathcal{D}|\theta) = \prod_{i=1}^I \frac{1}{\sqrt{2\pi\sigma^2}} \exp \left\{ -\frac{e_i(\mathcal{D}, \theta)^2}{2\sigma^2} \right\} \quad (9)$$

168 where $e_i(\mathcal{D}, \theta)$ are the residuals of the model given the parameters, and the evidence. In the case of
 169 the interpolation, the residuals correspond to the observation error $\varepsilon^{(o)}$ (equation 3). In the case of
 170 the NODE approximation, they correspond to the process error $\varepsilon^{(p)}$ (equation 7). I is the number

171 of data points, either observations in the case of the interpolation, or interpolated points in the case
 172 of the NODE fitting.

173 The prior probability density functions for the parameters are given by

$$p(\theta) = \prod_{j=1}^J \frac{1}{\sqrt{2\pi}\delta_j^2} \exp \left\{ -\frac{\theta_j^2}{2\delta_j^2} \right\} \quad (10)$$

174 where J is the number of parameters in the models. The parameter δ_j controls the dispersion of the
 175 priors, and thereby the complexity/level of constraint of the model.

176 There is no standard approach for choosing δ . Low values of dispersion may increase constraint
 177 on parameters too drastically, which would lead to underfitting, and result in a reduction of the
 178 variance of parameter estimates and bias mean estimates towards 0. In contrast, too high values of
 179 dispersion may lead to overfitting, by allowing for more complex shapes. To account for this, we
 180 optimise the models on the second-level of inference. This means that we are finding the optimal
 181 value of δ , in addition to optimising the model parameters. We do this by optimising the marginal
 182 posterior density of the parameters, obtained by averaging out δ following a modification of the
 183 approach developed by Cawley and Talbot (Cawley and Talbot 2007). This yields the following
 184 expression for the marginal log posterior density of the parameters

$$\log P(\theta|\mathcal{D}) \propto -\frac{I}{2} \log \left(1 + \sum_{i=1}^I e_i(\mathcal{D}, \theta)^2 \right) - \frac{J}{2} \log \left(1 + \sum_{j=1}^J \theta_j^2 \right) \quad (11)$$

$$\log P(\Omega|\mathcal{D}) \propto -\frac{I}{2} \log \left(1 + \sum_{i=1}^I \left(\varepsilon_i^{(o)} \right)^2 \right) - \frac{J}{2} \log \left(1 + \sum_{j=1}^J \Omega_j^2 \right) \quad (12)$$

$$\log p(\beta|\Omega) \propto -\frac{1}{2} \sum_{i=1}^I \left(\frac{\varepsilon_i^{(p)}}{\sigma} \right)^2 - \frac{1}{2} \sum_{j=1}^J \left(\frac{\beta_j}{\delta_j} \right)^2 \quad (13)$$

185 which amounts to optimising the log of the sum of squared residuals rather than the sum of squared
 186 residuals. $P(\theta|\mathcal{D})$ designates the marginal posterior distribution. More details on how to derive this
 187 expression from equation (8) can be found in a supplementary file (See supplementary A).

188 Finally, we estimate uncertainty in parameter values through anchor sampling, which produces ap-
 189 proximate Bayesian estimates of the posterior distribution of the parameters (Pearce et al. 2018).
 190 The technique is simple in that it requires sampling a parameter vector from the prior distribu-
 191 tions, and then optimising the posterior distribution from this starting point. By repeatedly taking
 192 samples, the sampled distribution approaches the posterior distribution and provides estimates and
 193 error around the quantities that can be derived from the models. The expectation of the quantities
 194 can then be approached by computing the mean of the approximated posterior distributions. The
 195 great strength of this approach is that it is unlikely to get stuck in local maxima and provides a
 196 more robust optimisation of the posterior. In this study, we took 100 posterior samples for each
 197 time series, namely a hundred samples for the interpolation, and another hundred for the fitting
 198 of the NODE. The initial value of the parameters were picked from a random normal distribution
 199 with parameters $\sigma \geq 0.4$, which prevented underfitting the time series. We insured that there was

200 moderate temporal autocorrelation and normality by visualising the residuals of the models. We
201 also insured that the results were repeatable by running the entire fitting process a second time. We
202 did not perform cross validation of results as we were only interested in estimating effects within
203 the time series considered, rather than predicting future time steps.

204 **2.4 Model analysis**

205 We analyse the shape of the per-capita growth rates to recover the interaction between the three
206 species in the system. In particular, we look at the effect and contribution of each species to the
207 dynamics of the other. The effect is computed as the sensitivity (i.e. the gradient) of the per-capita
208 growth rate of a given species with respect to the density of the other species. The contribution is
209 computed following the Geber method (Hairston et al. 2005), which comes down to multiplying
210 the dynamics of a variable by its effects on the other variables. We further compute the importance
211 of a species in driving the dynamics of another by computing its relative contribution compared to
212 other species at each time step. More details on how to recover these quantities can be found in our
213 previous study (Bonnaffé, Sheldon, and Coulson 2021).

214 **3 Case study**

215 **3.1 System**

216 We consider a three-species laboratory microcosm consisting of an algal prey (*Chlorella autroph-*
217 *ica*), a flagellate intermediate predator (*Oxyrrhis marina*), and a rotifer top predator (*Brachionus*

218 *plicatilis*). The algal prey is consumed by the intermediate and top predator, the top predator also
219 consumes the intermediate predator (Arndt 1993). The dynamics of this system, here the daily
220 change in the density of each species, were recorded in three replicated time series experiments
221 performed by Hiltunen and colleagues (Hiltunen et al. 2013, Fig. 1). The aim of their experiment
222 was to determine which type of population dynamics would arise in a system with two predators
223 competing for the same resource (the algae), where one predator (the rotifer) would also be able to
224 consume its competitor (the flagellate). According to their expectations, they found prey-predator
225 oscillations, where the lag between the density peaks of each species reflected their position in the
226 food web. Namely that the peak of algae preceded the flagellate peak, which itself preceded the
227 rotifer peak.

228 Their microcosms are close to true replicates in that environmental conditions, namely temperature,
229 salinity, and nutrient influx, were maintained constant, and initial conditions, that is the initial
230 density of each species, were shared across all replicates. In spite of that, they still found evidence
231 for algae evolution in some parts of the time series, which resulted in a shift of the dynamics from
232 fast prey-predator cycles to slower oscillations, similar to those documented in previous studies on
233 similar systems (Yoshida et al. 2003; Becks et al. 2010), even in lineages where genetic variation in
234 predator defense traits was eliminated at the start of the experiment. Consequently, the time series
235 that they reported are the ones that did not present evidence of evolution, and therefore displayed
236 purely ecological dynamics.

237 We use their time series because they describe a simple yet biologically realistic ecosystem, and

238 because the quality of the replication of their microcosm reduces as much as possible observational
239 and experimental error, and rules out environmental variation (Hiltunen et al. 2013). We digitised
240 these time series by extracting by hand the coordinates of every points in the referential of the axis
241 of the graph of the original study, and analysed them.

242 **3.2 Model specifications**

243 The aim of the modelling approach is to infer the drivers of the dynamics of each species from
244 the time series data. More specifically, we want to quantify the effect of a change in the density
245 of one species on the dynamics of the other species. In this way we can understand which, and
246 to what extent, species interactions drive population dynamics. To do this we use neural ordi-
247 nary differential equation (NODEs), which is a novel methodology allowing us to infer dynamical
248 processes non-parametrically from time series data (Bonnaffé, Sheldon, and Coulson 2021). We
249 choose this methodology over traditional approaches because it offers two advantages. The first
250 lies in the fact that NODEs approximate the dynamics of populations non-parametrically, and are
251 therefore not subject to incorrect model specifications (Jost and Ellner 2000; Adamson and Moro-
252 zov 2013). This is important as it offers an objective estimation of the inter-dependences between
253 state variables, and hence a reliable assessment of whether a species is contributing to the dynamics
254 of another. The second advantage is that it is a dynamical systems approach, which means that the
255 effects are estimated in a dynamically consistent system of ODEs (Bonnaffé, Sheldon, and Coulson
256 2021). This is useful because it accounts for the dynamical nature of the system, so that it includes
257 lag effects, not just direct correlations between variables.

258 We define a simple NODE system for the three-species system described previously

$$\begin{aligned}
\frac{dR}{dt} &= r_R(R, G, B, \beta_R)R \\
\frac{dG}{dt} &= r_G(R, G, B, \beta_G)G \\
\frac{dB}{dt} &= r_B(R, G, B, \beta_B)B
\end{aligned} \tag{14}$$

259 where dR/dt , dG/dt , and dB/dt denote the change in rotifer (R), algae (G), and flagellate (B)
260 density in continuous time. The per-capita growth rates r_R , r_G , and r_B are non-parametric functions
261 of the density R , G , B of each species. The shapes of the non-parametric functions are controlled
262 by the parameter vectors β_R , β_G , and β_B . Fitting the NODE system (1) amounts to finding the
263 parameter vectors, and thereby the per-capita growth rates, that best describe the changes in density
264 observed in the time series data.

265 Each non-parametric functions is an artificial neural network (ANN). ANNs are powerful mathe-
266 matical objects that can be trained to approximate the shape of dynamical processes (Funahashi and
267 Nakamura 1993; Chen and Chen 1993). For the sake of simplicity, we consider the simplest form
268 of an ANN which contains a single hidden layer, namely a single layer peceptron (SLP)

$$r_R = \sum_{i=1}^N \beta_i f_{\sigma}(\beta_{i0} + \beta_{i1}R + \beta_{i2}G + \beta_{i3}B) \tag{15}$$

269 which takes as input the density of each species R , G , and B , and output the corresponding per-
270 capita growth rate. The parameter vector β_R , β_G , β_B , contain the weight of the connections in the

ANNs. The SLP can be viewed as a weighted sum of basis functions f_{σ} of the state variables of the system. In this study we consider sigmoid basis functions, as they are commonly used and their capacity to approximate any continuous function is well established theoretically (Funahashi and Nakamura 1993). The number of units in the hidden layer N is chosen to be 10, as this is a commonly used number for systems of that size (e.g. Wu, Fukuhara, and Takeda 2005). More details regarding these models can be found in our previous work (Bonnaiffé, Sheldon, and Coulson 2021).

4 Results

We analyse sequentially the dynamics of each species, focussing on the amount of variation in per-capita growth rates explained by the NODE model, the overall direction, consistency, and importance of ecological interactions, and differences across replicates. Results are summarised in Table 1 and described in details for each species in the following section.

Drivers of top predator dynamics

Figure 2 presents the drivers of the dynamics of rotifer. The NODE approximation of the per-capita growth rate fits quite well the interpolated per-capita growth rate across all replicates (Fig. 2, A2 B2 and C2, $r^2 > 0.7$, Table 1). The analysis of effects reveals overall a positive effect of algae on rotifer growth in all replicates (Fig. 2, A3, B3, C3, green line). The intermediate predator has a positive effect on rotifer growth in replicates A and C only (Fig. 2, A3, B3, C3, blue line). We find positive intra-specific density-dependence in the first replicate only (Fig. 2, A3, red line). Overall,

all effects are consistent throughout the time series. The algae is the dominant driver of rotifer dynamics as it accounts for 55%, 93%, and 74% of the change in per-capita growth rates across the three replicates (Table 1, Fig. 2, A5, B5, C5, green line).

Drivers of the prey dynamics

The per-capita growth rate of the algae is well explained by the NODE approximation (Fig. 3, A2, B2, C2, $r^2 > 0.8$, Table 1). Overall, rotifers have a negative impact on the growth of algae in all replicates (Fig. 3, A3, B3, C3, red line). We find evidence for negative density-dependence in replicate A and positive density-dependence in replicate B, but not in replicate C (Fig. 3, A3, B3, C3, green line). The intermediate predator has an overall negative effect on Algae only in replicate B (Fig. 3, B3, blue line). The main driver of algae dynamics is the rotifer population, which accounts for 58%, 44%, and 90% of the change in algae per-capita growth rate across the three replicates. Density-dependence, however, plays a role in replicate A and B, with 40% and 24% of total change in growth, respectively (Table 1). The intermediate predator contributes only to algae growth in replicate B, accounting for 32% change in growth (Table 1). Overall, effects are found to be consistent throughout the time series except in replicate B (Fig. 3, B3), where effects vary in complicated ways, leading to a period in the time series where the algae is mostly driven by the intermediate predator and positive density-dependence, and less impacted by the top predator (Fig. 3, B5, from time 3 to 7.5).

Drivers of the intermediate predator dynamics

The per-capita growth rate of the intermediate predator is quite well captured by the NODE approx-

310 imation (Fig. 4, A2, B2, C2, $r^2 > 0.7$, Table 1). The intermediate predator is mainly negatively
311 affected by the rotifer population (Fig. 4, A3, B3, C3, red line). The algae has a negative effect
312 on flagellate growth in replicate A, and a positive one in replicate B (Fig. 4, A3, B3, green line).
313 The rotifer predator dynamics accounts for 78%, 62%, 91% of the change in the flagellate growth
314 rate, and the algae 20% and 37% in replicate A and B, respectively (Table 1, Fig. 4, A5, B5, C5).
315 Overall, effects are consistent throughout the time series.

316 **5 Discussion**

317 Our ability to generalise dynamical processes and patterns across populations and communities is
318 limited by the complexity of the processes, differences in environments, and incomplete and/or
319 erroneous observations. It remains unclear to what extent generalisation would be possible if we
320 overcame these limitations. We tackle this question by looking at the consistency of dynamical
321 patterns across three replicated runs of a simple three-species community, hosted in identical en-
322 vironmental conditions in the lab. We expected to find consistency in the drivers of population
323 dynamics, both in time and across replicates, and thereby demonstrate that generalisation of dy-
324 namical processes may be possible if the system states were well-observed and environmental
325 conditions were known. To verify this expectation we (1) characterised the amount of variation in
326 per-capita growth rates that is explainable deterministically, (2) quantified the direction, strength,
327 and importance of ecological interactions for the growth of each population, and (3) described how
328 these varied in time and across replicates. Our results are summarised in Figure 5. We find that

329 only the effect of algae on rotifer ($G \rightarrow R$), and that of rotifer on algae ($R \rightarrow G$) and flagellate
330 ($R \rightarrow B$) are conserved across the replicates. We find strong variation in the direction and impor-
331 tance of intra-specific density-dependence in rotifer ($R \rightarrow R$) and algae ($G \rightarrow G$) growth across the
332 three replicates. The role played by the intermediate predator in the system was also different in
333 all replicates, in that it only contributed substantially to the dynamics of the algae in replicate B
334 ($B \rightarrow G$), and was either negatively, positively, or not affected by the algae ($G \rightarrow B$). Overall, this
335 shows that the dominant interactions are conserved across replicates, but that minor interactions
336 vary substantially in importance and effect. Furthermore, we find that these dynamical processes
337 are more consistent in time within a system, than across replicates. Our results demonstrate that
338 because of partially generalisable dynamical processes, dynamical patterns may not be generalis-
339 able across systems, even with limited observation error and when environmental conditions and
340 community structure are conserved.

341 Overall, our results are consistent with the biology of the system. The rotifer top-predator is found
342 to have a strong negative impact on the two other species, in spite of variation in prey preference
343 across replicates. This is consistent with previous study which have established the importance
344 of rotifers for top-down control of flagellate and algal populations (Arndt 1993; Hiltunen et al.
345 2013). What is more suprising is the positive intra-specific density-dependence in the growth rate
346 of the rotifer population in replicate A. This implies that the population of rotifer grows more at
347 high density. This might be explained by various biological mechanisms, such as cannibalism
348 (Gilbert 1976), though evidence remains limited in the *Brachionus* genus, or higher mating success

349 at high density (Snell and Garman 1986). Similarly, the algae shows signs of positive intra-specific
350 density-dependence in replicate B, though this effect remains confined to a brief period in the time
351 series. This may be due to a higher chance of evading predators at high-density. This shows that the
352 NODEs approach used here recovers results consistent with existing knowledge, but also identify
353 subtle, more intriguing dynamical processes.

354 What might be the drivers of differences in the dynamical processes across these three replicates?
355 One of the main source of variation in dynamics may be differences in the intrinsic structure of
356 populations, such as variation in traits influencing intra- and inter-specific interactions which may
357 lead to different dynamics (Yoshida et al. 2003; Yoshida et al. 2007; De Meester et al. 2019;
358 Bruijning, Jongejans, and Turcotte 2019). Differences in the phenotypic structure may be due to
359 unaccounted variation in initial conditions (Becks et al. 2010), or variation that developed through-
360 out time as a result of evolution (e.g. Yoshida et al. 2003; Yoshida et al. 2007). In particular, the
361 algae in this system is prone to evolve a predator defence behaviour, by forming clumps, which
362 reduce predation risk (Yoshida et al. 2003; Hiltunen et al. 2013). In their original paper, the authors
363 limited the initial genetic diversity in the algae and focussed on replicates which did not display
364 evidence of evolution, in an attempt to limit the impact of initial variation in phenotypic structure,
365 and of evolution, on the dynamics (Hiltunen et al. 2013). In spite of that, evolution may not be
366 eliminated completely, thus variation in traits governing the interactions between the species in
367 the system may still have developed during the experiment, and led to changes in the dynamical
368 processes across replicates. This would further be consistent with results from Yoshida and col-

leagues, who showed that evolution of prey defense could lead to ecological dynamics inconsistent with the known trophic interactions (Yoshida et al. 2007). Becks and colleagues also showed that small changes in the initial genotypic diversity could lead to drastically different eco-evolutionary dynamics (Becks et al. 2010). Our study hence reinforces the idea that rapid evolution may prevent generalisation of dynamical processes (Ezard, Côté, and Pelletier 2009; De Meester et al. 2019), and further suggests that this may also be the case in simple systems with limited environmental variation and opportunity for evolution.

Alternatively, stochasticity may be a major driver of differences across systems (Dallas et al. 2021). First, stochasticity in initial conditions, arising from the sampling of the communities of each replicate, could introduce differences in the interactions between the three populations. Second, stochasticity in the population dynamics themselves may result in different changes in density levels in communities that are otherwise identical. Because our modelling approach is deterministic, it does not directly provide an estimate of the total variation explained by stochasticity. Our modelling approach decomposes the variation in the data into observation and process error (Calder et al. 2003). First, the interpolation step introduces residual observation error, namely variation that is not captured by the interpolation. Second, the fitting of the NODE to the interpolation introduces residual process error, which is variation in the observation model that is not explained by the process modelled by the NODE. Stochasticity in the dynamics could explain the observation and process residual error (Calder et al. 2003), while stochasticity in initial conditions can only influence differences across replicates. Yet, we find relatively small process and observation error ($> 70\%$

389 of variance explained). So that, the dynamics of the three species are well explained by relatively
390 simple linear deterministic effects between the state variables, which means that though dynamical
391 processes differ across replicates they are reasonably consistent in time within each system. This
392 suggests that stochasticity in dynamics plays a minor role in driving differences in dynamics across
393 replicates, compared to stochasticity in initial conditions. In order to quantify this, we would need
394 to estimate the influence of stochasticity directly. This can be done by modelling explicitly the
395 random distribution of model parameters that underpin the dynamics of populations, which would
396 then inform us about the importance of stochasticity driven by variation at the individual-level (Fox
397 and Kendall 2002). Additionally, we could model stochasticity explicitly in the model with neural
398 stochastic differential equations, which would allow us to separate the amount of change explain-
399 able by the deterministic part of the model, from demographic stochasticity, at each time step (Jia
400 and Benson 2019).

401 Finally, we cannot exclude the potential contribution of unobserved variables that were not moni-
402 tored during the experiment, such as variation in nutrient levels in the chemostat, and which may
403 also lead to differences in the predation and intra-specific interactions across systems (e.g. Bonsall,
404 Van Der Meijden, and Crawley 2003; Fussmann and Blasius 2005; Posey, Alphin, and Cahoon
405 2006).

406 Should we expect limited generalisability of dynamics across systems, even if the complexity of
407 the process is properly captured, environmental conditions known, and the system well-observed?
408 A similar study, that inferred dynamical processes consistency from replicated time series of a

409 simple rotifer system, found substantial variation in vital rates across replicates (Rosenbaum et al.
410 2019), also pointing at a low generalisability of dynamical processes. Yet, the level of replication
411 of the time series of their studies was not as stringent as that of the time series we considered,
412 which leaves room for variability in dynamics to be caused by differences in experimental setup,
413 population history, initial densities. Bruijning and colleagues also found substantial variation in
414 vital rates across clones in a replicated system of aphids, showing that slight phenotypic variations
415 can change the population dynamics, all else being equal (Bruijning, Jongejans, and Turcotte 2019).
416 This phenomenon is likely to be even more important in more complicated systems and in a natural
417 setting where most variables are unobserved, which poses a problem for the generalisation of results
418 across studies and systems (De Meester et al. 2019). How can we expect to generalise dynamics
419 across real systems if we are not able to do so in artificial systems? Overall, our study reinforces
420 the view that general inferences should not be drawn from a single system, and that more efforts
421 are required to distinguish dynamical patterns that are conserved across systems from idiosyncratic
422 ones.

423 Can we trust our models then if they are doomed to provide partly idiosyncratic answers? Our
424 study demonstrates that processes can vary substantially across replicates, so that there may hence
425 not be a single suitable functional form and parametrisation to model them (Lawton 1999). Yet,
426 most of the work to date has involved fitting parametric models to time series data (e.g. Bruijning,
427 Jongejans, and Turcotte 2019; Pontarp, Brännström, and Petchey 2019; Rosenbaum et al. 2019),
428 which provide a very narrow view of the range of possible functions to describe the biological

429 processes at play (Jost and Ellner 2000; Adamson and Morozov 2013). These models are subjective
430 by nature (Jost and Ellner 2000; Adamson and Morozov 2013), and hence not generalisable, so that
431 they greatly reduce our chance at identifying dynamical processes that are idiosyncratic, and those
432 that are transferable.

433 What alternatives do we have then? We propose that NODEs are a suitable framework to study
434 dynamical processes, as they produce inferences that are free of model assumption and facilitate
435 comparison across studies and systems (Bonnaiffé, Sheldon, and Coulson 2021). In this sense, our
436 study already provides a potentially more objective depiction of dynamical processes than previous
437 work with parametric models. Furthermore, in this paper we overcame the practical challenges
438 of implementing NODEs by providing a computationally efficient fitting procedure, relying on
439 time series interpolation, and developed a model selection criterion robust to overfitting. Similar
440 approaches have been proposed in the past, for instance Ellner and colleagues developed a method
441 called gradient matching where they interpolated the data with cubic splines to which they fitted
442 the differential equations (Jost and Ellner 2000; Ellner, Seifu, and Smith 2002). Wu and colleagues
443 also relied on data interpolation of the data with ANNs to fit non-parametric approximations of
444 population vital rates (Wu, Fukuhara, and Takeda 2005). But the approaches were too challenging
445 and cumbersome to be implemented routinely, and were not used to tackle ecological interactions.
446 Overall, our work demonstrates the usefulness of NODEs for inferring ecological interactions from
447 count time series, which could readily be applied to a substantial pool of time series data.

448 **Conclusion**

449 Generalising dynamics across biological systems is hard because of the complexity of the dynam-
450 ical processes (e.g. ecological interactions), differences in environmental context, and monitoring
451 limitations. It remains unclear whether we could generalise dynamics if we properly modelled
452 complexity, controlled for environmental effects, and observed systems precisely. We addressed
453 this question by looking at the generalisability of dynamical processes across three replicated time
454 series of a three-species system, using the novel framework of NODEs. We found that only the
455 dominant interactions were conserved across the three time series, namely that between the algae
456 and the rotifer, while the role of the intermediate predator varied substantially. Our results hence
457 suggest that generalisation may not seem possible, even in simple system with no environmental
458 variation. Given previous work in this system, the main cause of differences across replicates may
459 be evolution in prey defence traits. We conclude that more work is required, using NODEs, to
460 identify dynamical patterns that are conserved and those that are idiosyncratic across a wider range
461 of systems.

462 **Acknowledgments**

463 We thank warmly the Ecological and Evolutionary Dynamics Lab and Sheldon Lab Group at the
464 department of Zoology for their feedback and support. We thank Ben Sheldon for insightful sug-
465 gestions on early versions of the work. The work was supported by the Oxford-Oxitec scholarship
466 and the NERC DTP.

467 **Data accessibility**

468 All data and code will be made fully available at <https://github.com/WillemBonnafe/NODER/rotifer>.

469 **Statement of authorship**

470 Willem Bonnaffé designed the method, performed the analysis, wrote the manuscript; Tim Coulson
471 led investigations, provided input for the manuscript, commented on the manuscript.

472 **References**

- 473 Adamson, M. W. and A. Y. Morozov (2013). “When can we trust our model predictions? Un-
474 earthing structural sensitivity in biological systems”. In: *Proceedings of the Royal Society A:
475 Mathematical, Physical and Engineering Sciences* 469.2149, pp. 1–19.
- 476 Arndt, H. (1993). “Rotifers as predators on components of the microbial web (bacteria, heterotrophic
477 flagellates, ciliates) - a review”. In: *Hydrobiologia* 255-256.1, pp. 231–246.
- 478 Becks, L., S. P. Ellner, L. E. Jones, and N. G. J. Hairston (2010). “Reduction of adaptive ge-
479 netic diversity radically alters eco-evolutionary community dynamics”. In: *Ecology Letters* 13.8,
480 pp. 989–997.
- 481 – (2012). “The functional genomics of an eco-evolutionary feedback loop: Linking gene expres-
482 sion, trait evolution, and community dynamics”. In: *Ecology Letters* 15.5, pp. 492–501.
- 483 Bonnaffé, W., A. Danet, S. Legendre, and E. Edeline (2021). “Comparison of size-structured and
484 species-level trophic networks reveals antagonistic effects of temperature on vertical trophic
485 diversity at the population and species level”. In: *Oikos* 130.8, pp. 1297–1309.

486 Bonnaffé, W., B. C. Sheldon, and T. Coulson (2021). “Neural ordinary differential equations for
487 ecological and evolutionary time series analysis”. In: *Methods in Ecology and Evolution* 2, pp. 1–
488 46.

489 Bonsall, M. B., E. Van Der Meijden, and M. J. Crawley (2003). “Contrasting dynamics in the same
490 plant-herbivore interaction”. In: *Proceedings of the National Academy of Sciences of the United*
491 *States of America* 100.25, pp. 14932–14936.

492 Bruijning, M., E. Jongejans, and M. M. Turcotte (2019). “Demographic responses underlying eco-
493 evolutionary dynamics as revealed with inverse modelling”. In: *Journal of Animal Ecology* 88.5,
494 pp. 768–779.

495 Calder, C., M. Lavine, P. Müller, and J. S. Clark (2003). “Incorporating multiple sources of stochas-
496 ticity into dynamic population models”. In: *Ecology* 84.6, pp. 1395–1402.

497 Cawley, G. C. and N. L. C. Talbot (2007). “Preventing over-fitting during model selection via
498 bayesian regularisation of the hyper-parameters”. In: *Journal of Machine Learning Research* 8,
499 pp. 841–861.

500 Chen, T. and H. Chen (1993). “Approximations of Continuous Functionals by Neural Networks
501 with Application to Dynamic Systems”. In: *IEEE Transactions on Neural Networks* 4.6, pp. 910–
502 918.

503 Dallas, T., B. A. Melbourne, G. Legault, and A. Hastings (2021). “Initial abundance and stochas-
504 ticity influence competitive outcome in communities”. In: *Journal of Animal Ecology*, pp. 1–
505 26.

506 De Meester, L. et al. (2019). “Analysing eco-evolutionary dynamics—The challenging complexity
507 of the real world”. In: *Functional Ecology* 33.1, pp. 43–59.

508 Demyanov, V., S. N. Wood, and T. J. Kedwards (2006). “Improving ecological impact assessment
509 by statistical data synthesis using process-based models”. In: *Journal of the Royal Statistical*
510 *Society. Series C: Applied Statistics* 55.1, pp. 41–62.

511 Ellner, S. P., Y. Seifu, and R. H. Smith (2002). “Fitting Population Dynamic Models to Time-Series
512 Data by Gradient Matching”. In: *Ecology* 83.8, p. 2256.

513 Ezard, T. H. G., S. D. Côté, and F. Pelletier (2009). “Eco-evolutionary dynamics: Disentangling
514 phenotypic, environmental and population fluctuations”. In: *Philosophical Transactions of the*
515 *Royal Society B: Biological Sciences* 364.1523, pp. 1491–1498.

516 Fox, G. A. and B. E. Kendall (2002). “Demographic stochasticity and the variance reduction ef-
517 fect”. In: *Ecology* 83.7, pp. 1928–1934.

518 Funahashi, K.-i. and Y. Nakamura (1993). “Approximation of dynamical systems by continuous
519 time recurrent neural networks”. In: *Neural Networks* 6.6, pp. 801–806.

520 Fussmann, G. F. and B. Blasius (2005). “Community response to enrichment is highly sensitive to
521 model structure”. In: *Biology Letters* 1.1, pp. 9–12.

522 Gamelon, M. et al. (2019). “Accounting for interspecific competition and age structure in demo-
523 graphic analyses of density dependence improves predictions of fluctuations in population size”.
524 In: *Ecology Letters* 22.5, pp. 797–806.

525 Gilbert, J. J. (1976). “Selective cannibalism in the rotifer *Asplanchna sieboldi*: Contact recognition
526 of morphotype and clone”. In: *Proceedings of the National Academy of Sciences* 73.9, pp. 3233–
527 3237.

528 Gross, K., A. R. Ives, and E. V. Nordheim (2005). “Estimating fluctuating vital rates from time-
529 series data: A case study of aphid biocontrol”. In: *Ecology* 86.3, pp. 740–752.

530 Hairston, N. G. J., S. P. Ellner, M. A. Geber, T. Yoshida, and J. A. Fox (2005). “Rapid evolution and
531 the convergence of ecological and evolutionary time”. In: *Ecology Letters* 8.10, pp. 1114–1127.

532 Hiltunen, T., L. E. Jones, S. P. Ellner, and N. G. J. Hairston (2013). “Temporal dynamics of a simple
533 community with intraguild predation: an experimental test”. In: *Ecology* 94.4, pp. 773–779.

534 Jia, J. and A. R. Benson (2019). “Neural jump stochastic differential equations”. In: *Advances in*
535 *Neural Information Processing Systems* 32.NeurIPS.

536 Jost, C. and S. P. Ellner (2000). “Testing for predator dependence in predator-prey dynamics: A
537 non-parametric approach”. In: *Proceedings of the Royal Society B: Biological Sciences* 267.1453,
538 pp. 1611–1620.

539 Kendall, B. E. et al. (2005). “Population cycles in the pine looper moth: Dynamical tests of mech-
540 anistic hypotheses”. In: *Ecological Monographs* 75.2, pp. 259–276.

541 Lawton, J. H. (1999). “Are There General Laws in Ecology ?” In: *Oikos* 84.2, pp. 177–192.

542 Pearce, T., F. Leibfried, A. Brintrup, M. Zaki, and A. Neely (2018). “Uncertainty in Neural Net-
543 works: Approximately Bayesian Ensembling”. In: *arXiv*, pp. 1–10.

544 Pontarp, M., Å. Brännström, and O. L. Petchey (2019). “Inferring community assembly processes
545 from macroscopic patterns using dynamic eco-evolutionary models and Approximate Bayesian
546 Computation (ABC)”. In: *Methods in Ecology and Evolution* 10.4, pp. 450–460.

547 Posey, M. H., T. D. Alphin, and L. Cahoon (2006). “Benthic community responses to nutrient en-
548 richment and predator exclusion: Influence of background nutrient concentrations and interactive
549 effects”. In: *Journal of Experimental Marine Biology and Ecology* 330.1, pp. 105–118.

550 Raeymaekers, J. A. M. et al. (2017). “Adaptive and non-adaptive divergence in a common land-
551 scape”. In: *Nature Communications* 8.1, pp. 1–8.

552 Reznick, D. N., H. Bryga, and J. A. Endler (1990). “Experimentally induced life-history evolution
553 in a natural population”. In: *Nature* 346.6282, pp. 357–359.

554 Rosenbaum, B., M. Raatz, G. Weithoff, G. F. Fussmann, and U. Gaedke (2019). “Estimating param-
555 eters from multiple time series of population dynamics using bayesian inference”. In: *Frontiers
556 in Ecology and Evolution* 6.234, pp. 1–14.

557 Shurin, J. B., J. L. Clasen, H. S. Greig, P. Kratina, and P. L. Thompson (2012). “Warming shifts
558 top-down and bottom-up control of pond food web structure and function.” In: *Philosophical
559 transactions of the Royal Society of London. Series B, Biological sciences* 367.1605, pp. 3008–
560 17.

561 Snell, T. W. and B. L. Garman (1986). “Encounter probabilities between male and female rotifers”.
562 In: *Journal of Experimental Marine Biology and Ecology* 97.3, pp. 221–230.

563 Thompson, C. E., E. B. Taylor, and J. D. Mcphail (1997). “Parallel Evolution of Lake-Stream
564 Pairs of Threespine Sticklebacks (*Gasterosteus*) Inferred from Mitochondrial DNA Variation”.
565 In: *Evolution* 51.6, pp. 1955–1965.

566 Wu, J., M. Fukuhara, and T. Takeda (2005). “Parameter estimation of an ecological system by a
567 neural network with residual minimization training”. In: *Ecological Modelling* 189.3-4, pp. 289–
568 304.

569 Yoshida, T., S. P. Ellner, L. E. Jones, B. J. M. Bohannan, R. E. Lenski, and N. G. J. Hairston (2007).
570 “Cryptic population dynamics: Rapid evolution masks trophic interactions”. In: *PLoS Biology*
571 5.9, pp. 1868–1879.

572 Yoshida, T., L. E. Jones, S. P. Ellner, G. F. Fussmann, and N. G. J. Hairston (2003). “Rapid evo-
573 lution drives ecological dynamics in a predator – prey system”. In: *Nature* 424.July, pp. 303–
574 306.

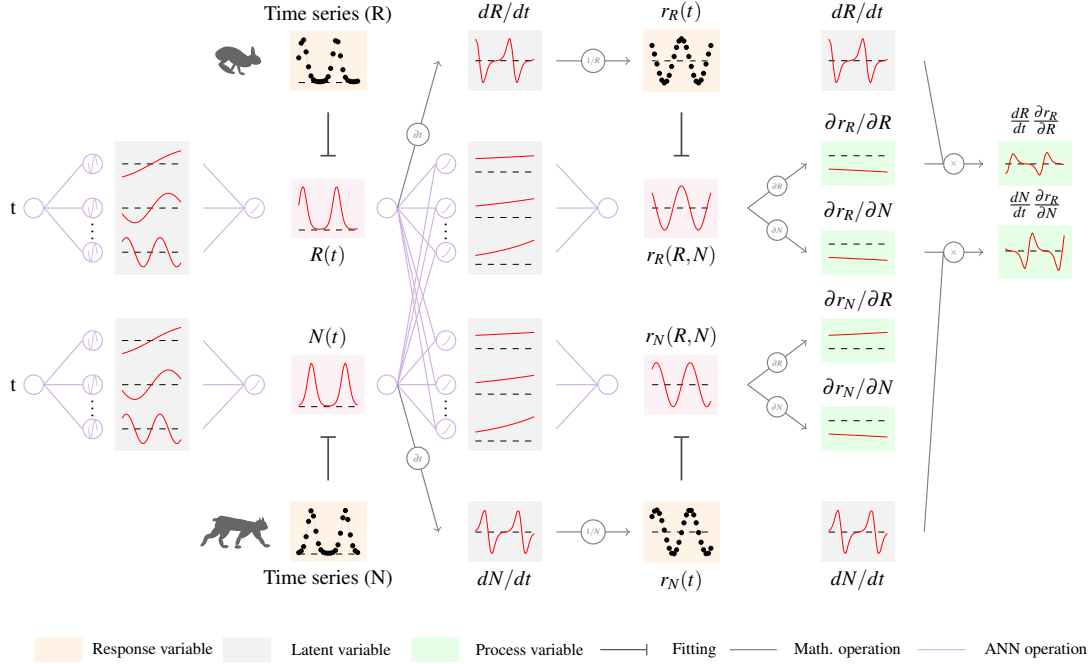


Figure 1: Overview of fitting neural ordinary differential equations by gradient matching

The first step is to compute a continuous time approximation (interpolation) of each state variables (e.g. resource $R(t)$ and predator $N(t)$). To do that we fit an ANN, that takes time as input, to each time series. Dynamics of populations can then be computed by taking the derivative of the ANN with respect to time, dR/dt and dN/dt . This provides an interpolation of the per-capita growth rate of each population, e.g. $r_R(t) = 1/R dR/dt$. In a second step, we approximate non-parametrically the per-capita growth rates with respect to the density of each populations, $r_R = s(R, N)$. To do that we fit an ANN, which takes as input the interpolated variables $R(t)$ and $N(t)$, to the interpolated per-capita growth rates $r_R(t)$ and $r_N(t)$. In a final step, we approximate the ecological interactions, by computing the sensitivity of the per-capita growth rates with respect to the density of each population, e.g. $E : N \rightarrow R = \partial r_R / \partial N$. We also compute the contribution of each species to the dynamics of the other by multiplying the dynamics of each variable with its effect on the growth rates (i.e. the Geber method), e.g. $C : N \rightarrow R = dN/dt \times \partial r_R / \partial N$.

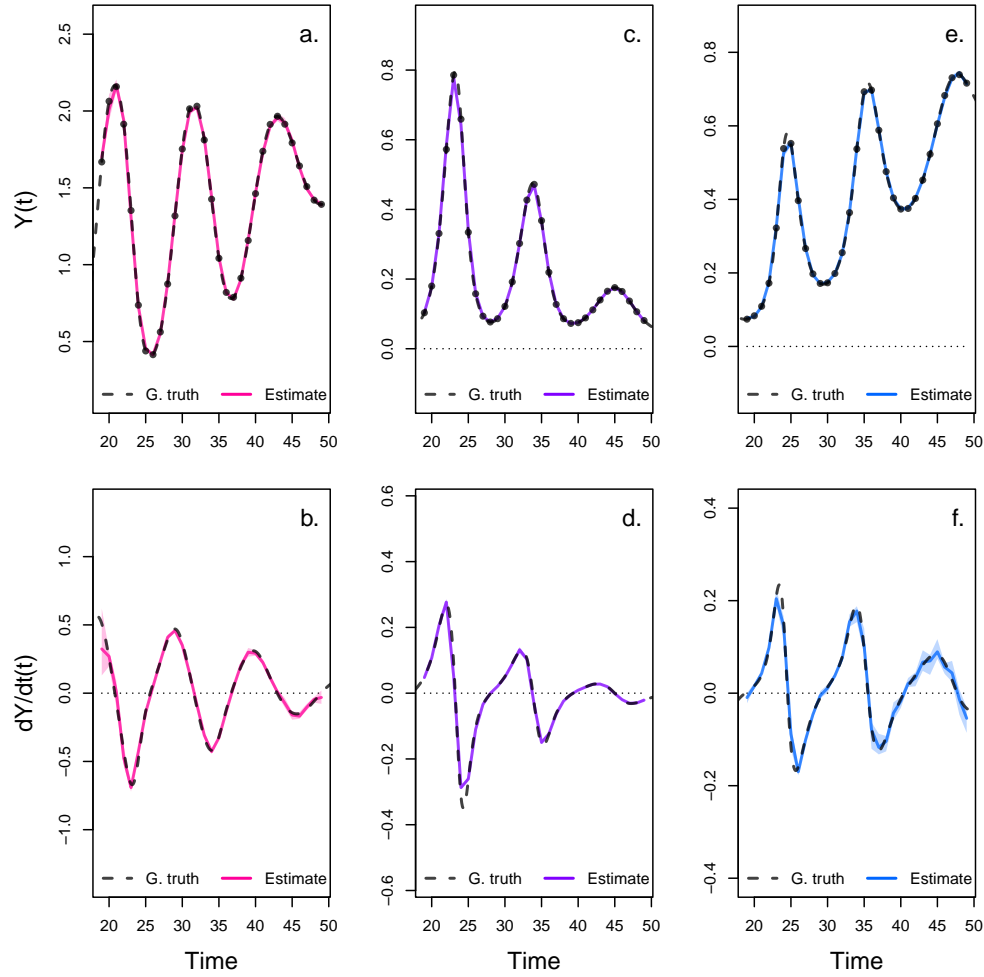


Figure 2: Interpolated density and dynamics of algae, flagellate, and rotifer in the artificial system. This figure corresponds to the first step in the overview figure. It shows the accuracy of the interpolated densities of algae (a.), flagellate (c.), and rotifer (e.). We obtain interpolated densities by fitting observed densities (black dots) with ANNs that take time as input. The observed densities were obtained by sampling a tri-trophic prey-predator ODE model at regular time steps. We then derive interpolated dynamics (b., d., f.) by computing the temporal derivative of the interpolated densities with respect to time. In all graphs, the dashed line represents the ground truth, namely trajectories generated by the ODE model. The solid lines correspond to the interpolations. The shaded area shows the 90% confidence interval, obtained by approximately sampling the marginal posterior distributions.

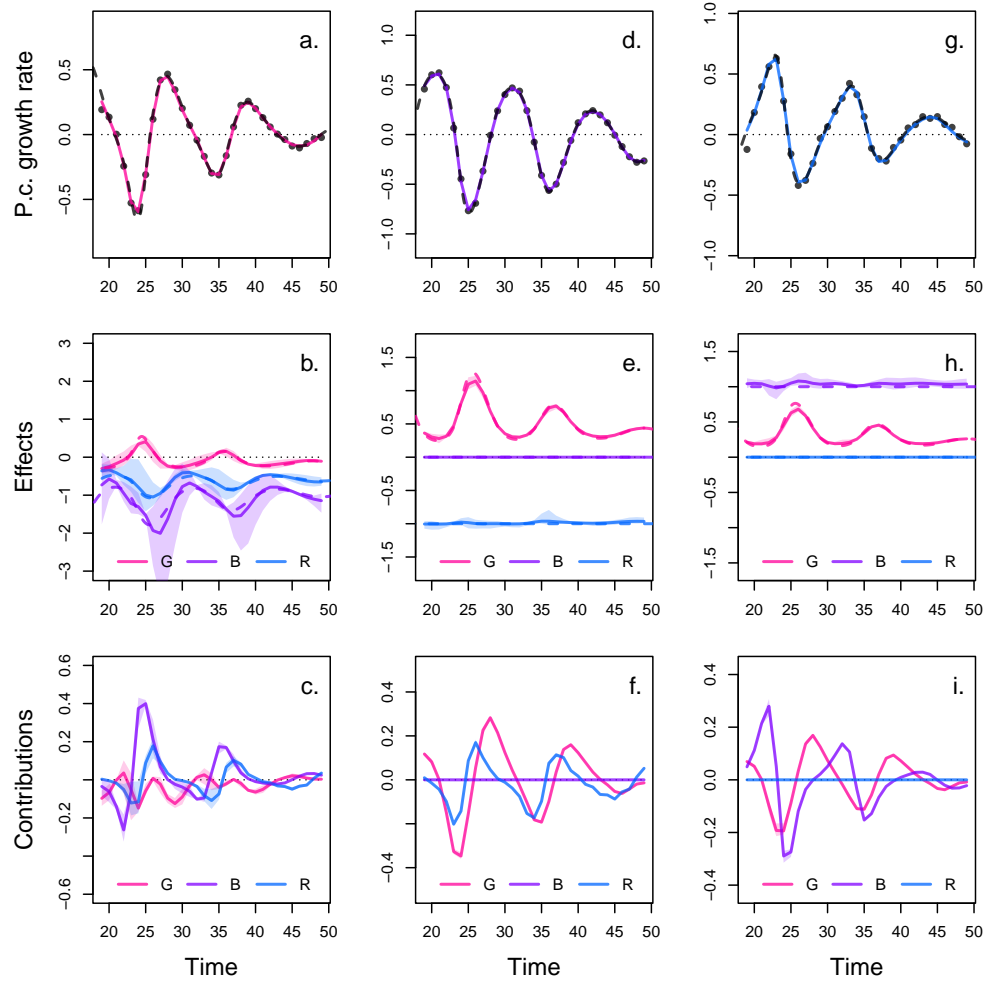


Figure 3: Drivers of dynamics of algae, flagellate, and rotifer in the artificial system. This figure corresponds to the second step in the overview figure. It displays the NODE non-parametric approximations of the per-capita growth rate of algae (a., b., c.), flagellate (d., e., f.), and rotifer (g., h., i.). We obtain the NODE approximations (a., d., g., solid line) by fitting the interpolated per-capita growth rates (black dots) with ANNs that take population densities as input. We then estimate the direction of ecological interactions (effects, b., e., h.) by computing the derivative of the NODE approximations with respect to each density. Finally, we compute the strength of ecological interactions (contributions, c., f., i.) by multiplying the interpolated dynamics of each population (fig. 1, b., d., f.) with its effects. Dashed lines correspond to ground truth, obtained from the original trajectories of the tri-trophic ODE model. The shaded area shows the 90% confidence interval, obtained by approximately sampling the posterior distributions.

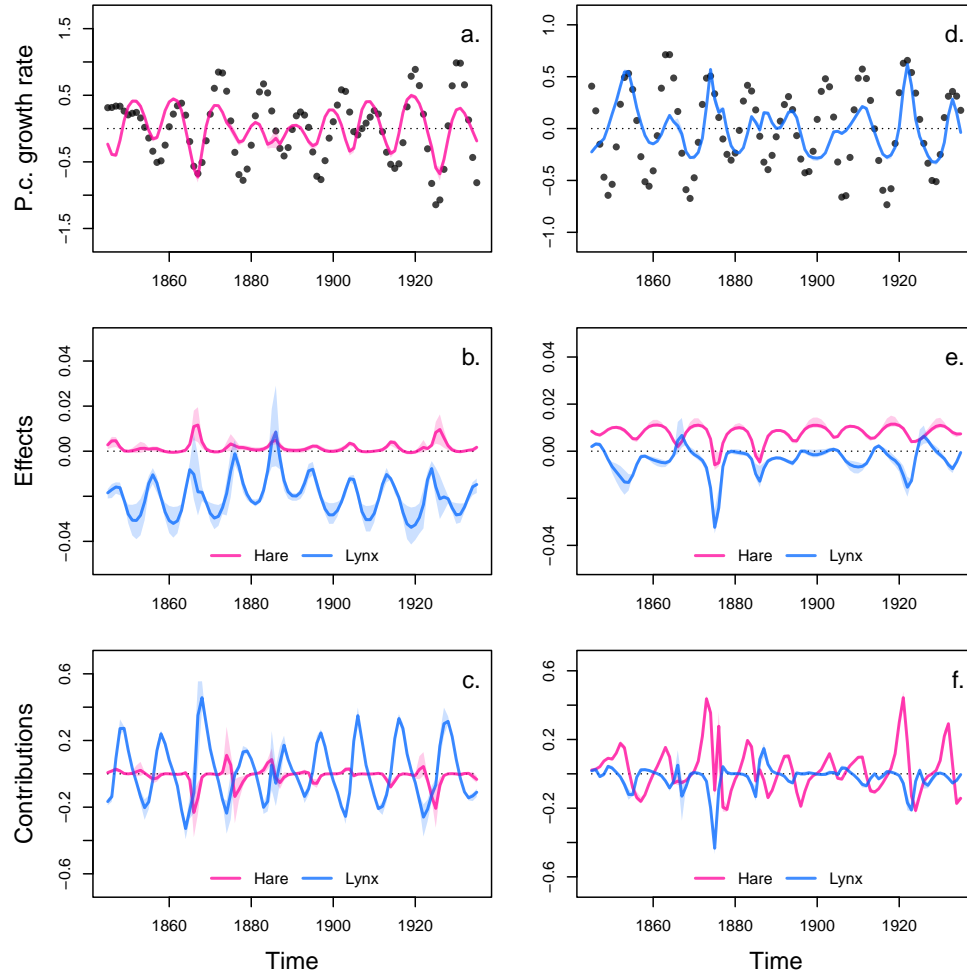


Figure 4: Drivers of dynamics of hare and lynx in the Odum and Barrett pelt count time series. This figure displays the NODE non-parametric approximations of the per-capita growth rate of hare (a., b., c.), and lynx (d., e., f.). We obtain the NODE approximations (a., d., solid line) by fitting the interpolated per-capita growth rates (black dots) with ANNs that take population densities as input. We then estimate the direction of ecological interactions (effects, b., e.) by computing the derivative of the NODE approximations with respect to each density. Finally, we compute the strength of ecological interactions (contributions, c., f.) by multiplying the interpolated dynamics of each population with its effects. The shaded area shows the 90% confidence interval, obtained by approximately sampling the posterior distributions.

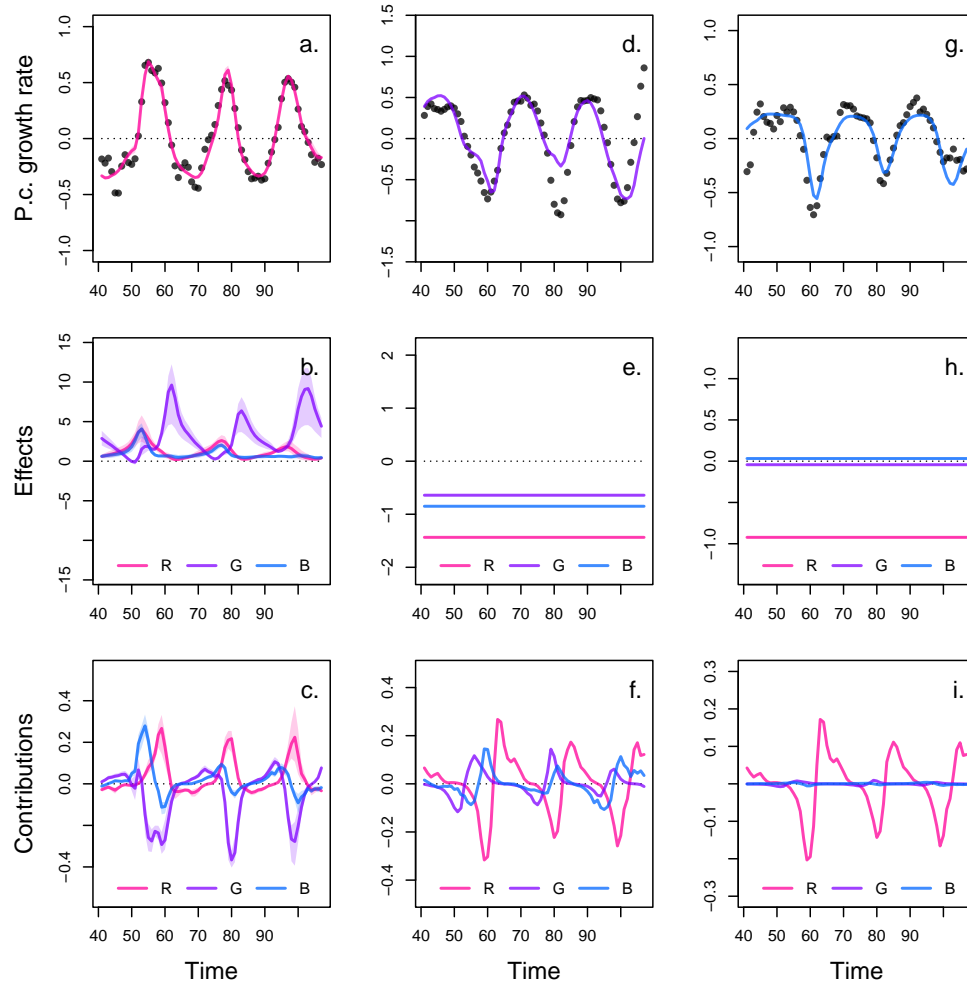


Figure 5: Drivers of dynamics of algae, flagellate, and rotifer in replicate A. This figure displays the NODE non-parametric approximations of the per-capita growth rate of algae (a., b., c.), flagellate (d., e., f.), and rotifer (g., h., i.). We obtain the NODE approximations (a., d., g., solid line) by fitting the interpolated per-capita growth rates (black dots) with ANNs that take population densities as input. We then estimate the direction of ecological interactions (effects, b., e., h.) by computing the derivative of the NODE approximations with respect to each density. Finally, we compute the strength of ecological interactions (contributions, c., f., i.) by multiplying the interpolated dynamics of each population with its effects. The shaded area shows the 90% confidence interval, obtained by approximately sampling the posterior distributions. The replicated time series were obtained by digitising the time series in Hiltunen et al. (2013).

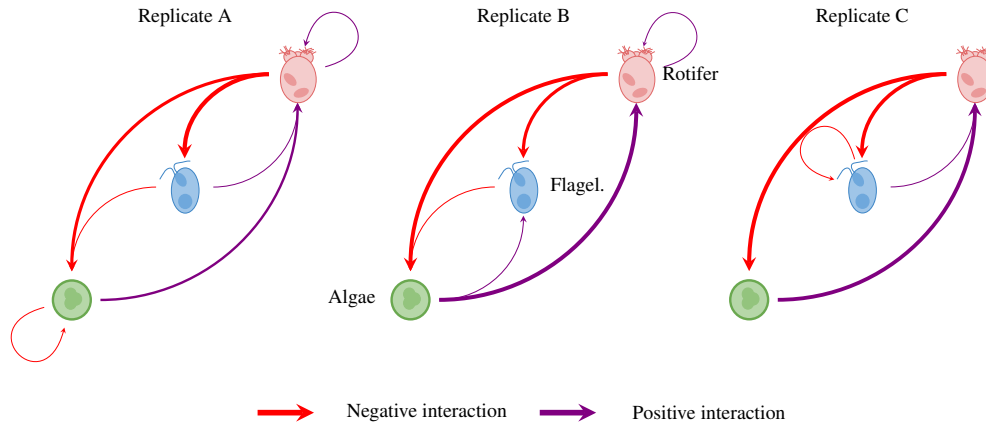


Figure 6: Interaction networks inferred from 3 replicated time series of algae, flagellate, and rotifers. This figure shows the direction and strength of ecological interactions inferred from 3 replicated sets of time series of algae, flagellate, and rotifer, using NODEs fitted by gradient matching. The replicates B and C were analysed in the same way as replicate A (see fig. 5 for details). Red and purple arrows correspond to negative or positive mean effects. We estimated mean effects by averaging effects (i.e. derivative of NODE approximated per-capita growth rates with respect to each population density) across the time series. The width of the arrows is proportional to the relative strength of the ecological interaction. We compute the relative strength as the % of total contributions attributable to either algae, flagellate, or rotifer, obtained from summing the square of contributions of each species throughout the time series. For instance in replicate A, the relative strength of the effect of rotifer on algae is found by summing the square of the red line in fig. 5 f., and computing the % of total contributions that it accounts for. We provide the value of the mean effects and relative strengths in Table 1. The replicated time series were obtained by digitising the time series in Hiltunen et al. (2013).

Table 1: Summary analysis. r^2 corresponds to the r squared of the NODE non-parametric approximation of the pre-capita growth rate compared to the interpolated per-capita growth rate for each of the three species. Mean effects are obtained by averaging the effect of one species on the growth rate of another throughout the time series. The % of total contributions is obtained by summing the square of contributions of one species density to the growth of the other at each time step throughout the time series, then by computing the proportion of total change that it accounts for.

		R	G	B
replicate A				
Mean effects	on R	0.27	0.77	0.97
	on G	-1.17	-0.44	-0.85
	on B	-0.78	0.04	0.03
% of total contributions	to R	0.08	0.48	0.44
	to G	0.75	0.08	0.17
	to B	1	0	0
replicate B				
Mean effects	on R	0.08	0.59	0.22
	on G	-1	0.05	-0.48
	on B	-0.47	0.14	-0.02
% of total contributions	to R	0.02	0.93	0.05
	to G	0.9	0	0.1
	to B	0.9	0.1	0
replicate C				
Mean effects	on R	-0.1	0.45	0.93
	on G	-1.76	-0.13	-0.12
	on B	-0.76	0.01	0.08
% of total contributions	to R	0.01	0.31	0.67
	to G	0.99	0.01	0
	to B	0.99	0	0.01

575 6 Supplementary

576 A Bayesian regularisation

577 In this section we describe how to derive the modified model selection criteria developed by Caw-
578 ley and Talbot (Cawley and Talbot 2007). Bayesian regularisation simply amounts to constraining
579 the values of the parameters in the model to be close to a desired value. Usually, parameters are
580 constrained by choosing normal priors centered about 0. In this case, the standard deviation of the
581 normal priors governs the range of values that the parameters can take, and hence constrains more
582 or less strongly the behaviour of the model (Cawley and Talbot 2007). Performing inference on the
583 second level means that we are trying to find the appropriate value of the dispersion of the priors,
584 in other words, the appropriate level of constraint on the model. In practice, choosing the level of
585 constraint is difficult, Cawley and Talbot hence developed a criterion to perform model selection
586 on the second level of inference. They proposed to optimise the marginal posterior distribution by
587 averaging out the dispersion of the priors. With an appropriate choice of prior, the dispersion can
588 be integrated out, leaving us with a formula for the posterior that only depends on the parameters
589 of the model,

$$\log P(\theta|\mathcal{D}) \propto \frac{I}{2} \log \left(\sum_{i=1}^I e_i(\mathcal{D}, \theta)^2 \right) + \frac{J}{2} \log \left(\sum_{j=1}^J \theta_j^2 \right) \quad (16)$$

590 where $P(\theta|\mathcal{D})$ denotes the marginal posterior density, \mathcal{D} denotes the evidence, I and J denote the

591 number of data points and parameters, respectively, e_i denote the residuals of the model, and θ
592 denote the parameters of the model. The construction is elegant because it is not sensitive to the
593 choice of prior hyperparameters, and simple as it amounts to optimising the log of the sum of
594 squares, rather than the sum of squares (in the case of normal ordinary least square).
595 The issue with this formula is that the marginal posterior density is infinity when the parameters
596 are 0, which leads to underfitting. In this paper we use a modified criterion, which corrects for that
597 problem

$$\log P(\theta|\mathcal{D}) \propto \frac{I}{2} \log \left(1 + \sum_{i=1}^I e_i(\mathcal{D}, \theta)^2 \right) + \frac{J}{2} \log \left(1 + \sum_{j=1}^J \theta_j^2 \right) \quad (17)$$

598 where the marginal posterior density depends only on the residuals of the model when the parame-
599 ters are equal to 0, and otherwise depends on both the parameters and the residuals. This construc-
600 tion can be obtained simply by assuming a gamma prior for the parameters $p(\xi) \propto \frac{1}{\xi} \exp\{-\xi\}$,
601 where ξ is the regularisation parameter, instead of the improper Jeffreys' prior that Cawley and
602 Talbot used in their original study, namely $p(\xi) \propto \frac{1}{\xi}$. The details of the integration of the posterior
603 distribution over ξ can be found in Cawley and Talbot's original paper.